ChemComm

COMMUNICATION

View Article Online
View Journal | View Issue

Cite this: *Chem. Commun.*, 2022, **58**, 11252

Received 31st May 2022,
Accepted 9th September 2022

DOI: 10.1039/d2cc03087j

rsc.li/chemcomm

Ionic encapsulation of a methanol carbonylation catalyst in a microporous metal–organic framework†

Samuel A. Ivko, [ac] Tom Bailey, [bc] Lee Brammer [c] and Anthony Haynes *[c]

The anionic rhodium complex *cis*-$[Rh(CO)_2I_2]^-$, active in the Monsanto process for acetic acid production, has been heterogenised *via* Coulombic interactions in the pores of a UiO-66-type metal–organic framework (MOF). The MOF-supported catalyst is active for the carbonylation of methanol and is recyclable, retaining its framework crystallinity following catalysis. Intermediates in the catalytic cycle observed by IR spectroscopy confirm the same mechanism as the established homogeneous process.

The bulk manufacture of acetic acid is an important industrial process with a demand for approximately 20 million tonnes per annum.[1] The majority of this demand is met *via* the catalytic carbonylation of methanol using homogeneous group 9 transition metal catalysts.[2] The rhodium/iodide catalysed Monsanto process was originally developed in the 1960s and produces acetic acid with very high selectivity (>99% based on MeOH). The catalytic cycle (Scheme 1) involves a series of anionic Rh iodocarbonyl complexes, beginning with *cis*-$[Rh(CO)_2I_2]^-$. This Rh(I) complex can also participate in a water–gas shift cycle *via* oxidation to the Rh(III) species, $[Rh(CO)_2I_4]^-$,[3] which is inactive for carbonylation and can degrade to give insoluble rhodium compounds. To maintain high catalytic activity and solubility, a relatively high water concentration (~10 wt%) is employed to suppress accumulation of inactive $[Rh(CO)_2I_4]^-$, but this increases the cost of drying the acetic acid product by distillation.[4] Homogeneous processes that operate at lower water concentration have been developed, including the Celanese AO Plus technology which employs a lithium iodide additive for the Rh catalyst,[5] and the iridium-based Cativa process developed by BP.[6,7]

The issues with catalyst activity and solubility can potentially be alleviated by heterogenisation of the metal complex on a solid support, which constrains the catalyst in the reactor. In the case of an anionic complex such as $[Rh(CO)_2I_2]^-$, a convenient approach, that maintains the primary coordination sphere of the metal complex, is to employ electrostatic (ion-pair) interactions with a cationic support. This approach was first used by Drago *et al.* who described the effective immobilisation of $[Rh(CO)_2I_2]^-$ on polymer supports based on *N*-methylated polyvinylpyridines and found carbonylation activity equal to the homogeneous system with minimal leaching.[8] This ionic attachment approach was later adopted in the Acetica™ process developed by Chiyoda/UOP, which attains rates comparable with the homogeneous system but requires lower water concentrations and can employ a higher catalyst loading due to the removal of solubility constraints.[9] Mechanistic studies on

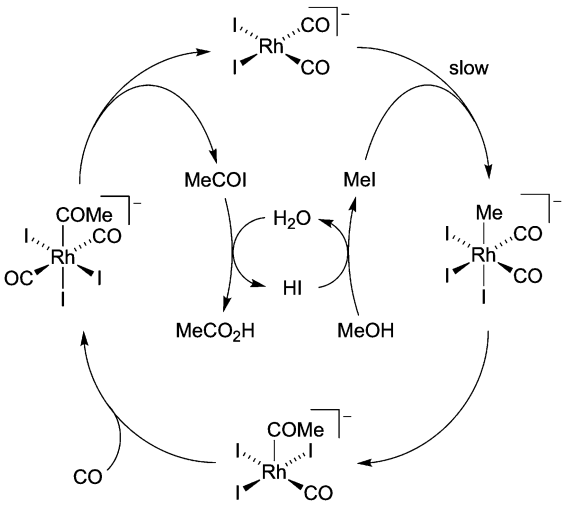

Scheme 1 Catalytic cycle for rhodium/iodide catalysed methanol carbonylation.

[a] *School of Chemistry, University of Birmingham, Birmingham B15 2TT, UK*
[b] *School of Chemical and Process Engineering, University of Leeds, Leeds LS2 9JT, UK*
[c] *Department of Chemistry, University of Sheffield, Sheffield S3 7HF, UK. E-mail: a.haynes@sheffield.ac.uk*

† Electronic supplementary information (ESI) available: Experimental details of synthesis and catalysis, additional characterisation data (^{1}H NMR; $^{13}C\{^1H\}$ CP-MAS NMR, PXRD with Pawley fits; N_2 volumetric adsorption). See DOI: https://doi.org/10.1039/d2cc03087j

related polymer-supported systems in our labs in Sheffield,[10] including a recent study using dispersible microporous nanoparticles,[11] have shown that the same catalytic cycle operates for the supported catalyst as in homogeneous solution phase.

Another class of materials that have received considerable recent attention for their potential as supports for catalyst heterogenisation are metal–organic frameworks (MOFs).[12–17] These crystalline, porous materials can incorporate well-defined catalytic sites and facilitate diffusion of reactants and products. The ionic attachment approach has been demonstrated most often with cationic complexes encapsulated in anionic MOFs, for example with Rh and Ir hydrogenation catalysts,[18–20] Ru metathesis catalysts[21–23] and others.[24–27] Alternatively, an anionic complex can be supported in a cationic MOF. For example, exchange of $[Co(CO)_4]^-$ with halide counter-ions in Cr-MIL-101 gave a supported catalyst that was effective for the carbonylation of epoxides.[28,29]

In relation to catalytic methanol carbonylation, Burgun *et al.* used a Mn(II)-based MOF with linkers containing bis(pyrazolyl)-methane units to coordinate $Rh(CO)_2^+$ moieties. The system showed activity for the carbonylation of MeBr[30] and single-crystal crystallographic studies mapped out a series of steps in a catalytic cycle involving *N*,*N*-chelated cationic Rh species. Interestingly, one of the materials characterised contained $[Rh(CO)_2Cl_2]^-$ as counter-ion. In this communication, we report the synthesis and characterisation of MOFs having a cationic framework into which the Monsanto carbonylation catalyst $[Rh(CO)_2I_2]^-$ is incorporated, and demonstrate activity for catalytic carbonylation of MeOH/MeI, as well as elucidating steps in the catalytic mechanism.

UiO-type MOFs[31] were selected as the platform for heterogenisation of the Rh catalyst. This family of MOFs is based on $[Zr_6(\mu_3\text{-}O)_4(\mu_3\text{-}OH)_4]^{12+}$ secondary building units (SBUs) with dicarboxylate linkers (*e.g.* benzene-1,4-dicarboxylate, BDC, in UiO-66). The exceptional thermal and chemical stability resulting from the hard acid-hard base interactions between the highly charged SBUs and carboxylate linkers make this family of MOFs attractive for post-synthetic modification[32,33] and catalytic applications.[34,35] Liang *et al.* recently reported a functionalised UiO-66-type MOF, $[Zr_6O_4(OH)_4(BDC\text{-}Im)_6]$ (BDC-Im = 2-(imidazol-1-yl)benzene-1,4-dicarboxylate), in which *N*-methylation of the pendant imidazolyl groups on the linkers gave a cationic framework with iodide counter-ions.[36] The aim of our study was to incorporate $[Rh(CO)_2I_2]^-$ as the counter-ion into MOFs of this type, enabling catalysis of carbonylation reactions within the confined pore space.

The imidazolyl-functionalised MOF, $[Zr_6O_4(OH)_4(BDC\text{-}Im)_6]$ was synthesised according to the procedure of Liang *et al.* (S2.4, ESI†).[36] For post-synthetic *N*-methylation of the imidazolyl groups, we found that higher conversion could be achieved in shorter reactions times by using microwave heating (85%, 1 h) rather than conventional heating (75%, 48 h) as determined by ^{1}H NMR spectroscopy following digestion in D_3PO_4/D_2O (Fig. S5, ESI†). Successful quaternisation was confirmed by solid-state CP-MAS $^{13}C\{^1H\}$ NMR, in which a new resonance was observed at 38 ppm, consistent with the methyl signal

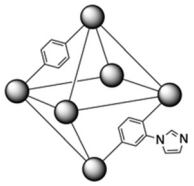

Fig. 1 Schematic structure of mixed-linker MOF **1**; grey spheres represent $[Zr_6(\mu_3\text{-}O)_4(\mu_3\text{-}OH)_4(CO_2)_{12}]$ units, connected by BDC or BDC-Im linkers.

observed in the solution-phase $^{13}C\{^1H\}$ NMR spectrum of the free quaternised linker, [H_2BDC-Im-Me][I] (synthesised independently) (Fig. S6, ESI†).

In order to increase the extent of quaternisation, we sought to reduce steric congestion in the MOF pores by employing a mixed-linker approach, incorporating both BDC and BDC-Im linkers (Fig. 1). A new MOF (**1**) was synthesised, using a 5 : 1 ratio of H_2BDC and H_2BDC-Im in the initial reaction mixture. Powder X-ray diffraction (PXRD) confirmed the synthesis of a UiO-66-type MOF as a single phase (Fig. 2a, Pawley fitting in Fig. S7, ESI†). The ^{1}H NMR spectrum of a sample of **1** digested in D_2O/NaOD (Fig. S9, ESI†) indicated presence of some modulator-induced acetate present as missing-linker defects in the final product, giving the formula $[Zr_6O_4(OH)_4(BDC)_{4.8}(BDC\text{-}Im)_{1.1}(OAc)_{0.1}]$ for **1**.

Reaction of **1** with MeI yielded $[Zr_6O_4(OH)_4(BDC)_{4.8}(BDC\text{-}Im\text{-}Me)_{1.1}(OAc)_{0.1}][I]_{1.1}$ **2** with 98% of the linker imidazolyl sites methylated (S2.7 and Fig. S12, ESI†), demonstrating a significantly higher conversion than for the single-linker MOF[36] and PXRD measurements demonstrate that **2** retains crystallinity (Fig. 2a, Pawley fitting in Fig. S10, ESI†). Volumetric N_2 gas sorption studies at 77 K (Fig. 2c and Table S1, ESI†) show that the surface area of **1** (1139 $m^2\ g^{-1}$) is ~8% lower than that of the parent UiO-66 (1238 $m^2\ g^{-1}$), synthesised in an analogous manner to **1**. A further 10% reduction in surface area occurs upon methylation to give **2**. The surface areas of **1** and **2**,

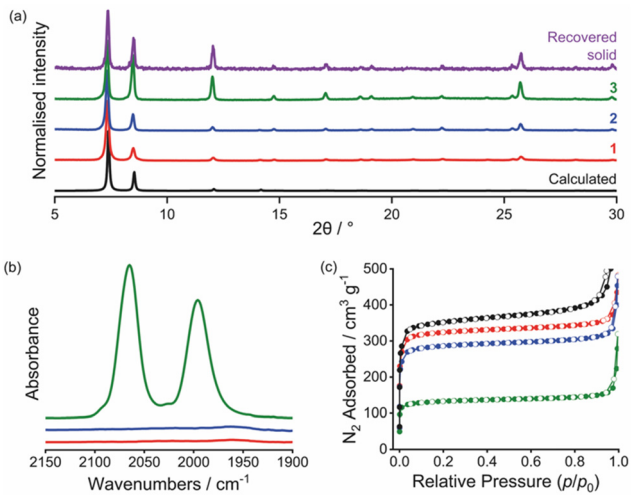

Fig. 2 (a) PXRD patterns (including calculated pattern of UiO-66 (black), and pattern of solid recovered after catalysis (purple)), (b) infrared spectra (KBr disc, ν(CO) region), and (c) nitrogen adsorption (filled) and desorption (open) isotherms at 77 K, for UiO-66 (black), **1** (red), **2** (blue) and **3** (green).

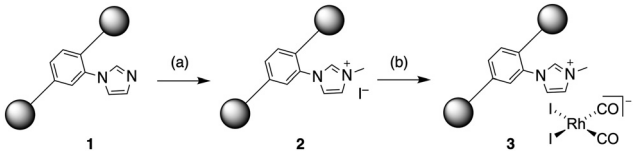

Scheme 2 Schematic illustration of post-synthetic quaternisation of **1** to form **2** and subsequent incorporation of Rh(I) complex to give **3**. Grey spheres represent $[Zr_6(\mu_3\text{-}O)_4(\mu_3\text{-}OH)_4(CO_2)_{12}]$ units. Only the functionalised BDC-Im linker is shown for clarity. (a) 4 M MeI in MeCN, microwave reactor, 120 °C 1 h, (b) $[Rh(CO)_2I]_2$ in dry *n*-hexane, CO atmosphere, RT 16 h.

however, are both higher than those reported by Liang *et al.*[36] for the single-linker analogues, $[Zr_6O_4(OH)_4(BDC\text{-}Im)_6]$ (538 $m^2\ g^{-1}$) and $[Zr_6O_4(OH)_4(BDC\text{-}Im)_{1.5}(BDC\text{-}Im\text{-}Me)_{4.5}][I]_{4.5}$ (328 $m^2\ g^{-1}$), indicating that the mixed-linker approach succeeds in reducing pore congestion and facilitating quaternisation of **1** to give **2**. The micropore volume also decreases in the order UiO-66 > **1** > **2** (Table S1, ESI†), suggesting that the pendant imidazolyl groups and I^- counter-ions occupy the micropores of the MOF.

Using a strategy analogous to that employed previously to generate polymer-supported $[Rh(CO)_2I_2]^-$,[10,11] a sample of **2** was treated with the iodide bridged rhodium dimer $[Rh(CO)_2I]_2$, which reacts with the I^- counter-ions in **2** (Scheme 2). The presence of a Rh(I) complex *cis*-$[Rh(CO)_2I_2]^-$ in the product **3** was confirmed by the presence of two ν(CO) absorptions at 2060 and 1986 cm^{-1} in the IR spectrum (Fig. 2b), very close to the ν(CO) bands for ^{n}Bu$_4$N$[Rh(CO)_2I_2]$ in MeOH solution (2060 and 1990 cm^{-1}).[37] The PXRD pattern for **3** (Fig. 2a) shows that crystallinity is retained and Pawley fitting (Fig. S13, ESI†) confirms no change in unit cell dimensions (Table S2, ESI†) indicating retention of framework integrity. Changes in relative diffraction intensities between patterns for **2** and **3** (Fig. 2a and Fig. S10, S13, ESI†) are indicative of the change in composition due to replacement of I^- anions by $[Rh(CO)_2I_2]^-$ anions within the framework pores. ICP-OES analysis confirmed the presence of rhodium (5 wt%) in the product which corresponds to stoichiometric uptake of Rh relative to the BDC-Im linker, giving the formula $[Zr_6O_4(OH)_4(BDC)_{4.8}(BDC\text{-}Im\text{-}Me)_{1.1}(OAc)_{0.1}][Rh(CO)_2I_2]_{1.1}$ for **3**. Volumetric N_2 gas sorption measurements showed a significantly smaller surface area and micropore volume for **3**, relative to **1** and **2**, indicating that the *cis*-$[Rh(CO)_2I_2]^-$ counter-ions occupy the micropores of the MOF.

In a control experiment, reaction of the non-quaternised MOF **1** with $[Rh(CO)_2I]_2$ gave a product that exhibited ν(CO) absorptions at 2075 cm^{-1} and 2007 cm^{-1} (Fig. S16, ESI†). The higher ν(CO) values indicate formation of a neutral rhodium dicarbonyl species, consistent with coordination of the imidazolyl nitrogen lone pair to a neutral $Rh(CO)_2I$ moiety[38] (rather than an ion-paired $[Rh(CO)_2I_2]^-$ anion, as in **3**).

As observed previously in polymeric systems, MOF-supported *cis*-$[Rh(CO)_2I_2]^-$ reacts with MeI in an analogous manner to the solution-phase catalyst (Scheme 1 and S2.10, ESI†). After soaking a sample of **3** in MeI overnight, the IR spectrum of the product contained one terminal ν(CO) band at 2060 cm^{-1}, as well as a broad band at around 1735 cm^{-1} (Fig. 3a). This is consistent with formation of the acetyl complex, $[Rh(CO)(COMe)I_3]^-$, resulting from oxidative addition of MeI to *cis*-$[Rh(CO)_2I_2]^-$, followed by rapid methyl migration, as observed in the homogeneous system.[39] After exposure of the solid product to CO gas (1 atm), the IR spectrum showed absorptions at 2088 and 1694 cm^{-1} (Fig. 3a), consistent with the dicarbonyl complex *trans*-$[Rh(CO)_2(COMe)I_3]^-$ also observed in solution.[40] Thus, the key organometallic intermediates from the homogeneous catalytic cycle shown in Scheme 1 are also observed in the MOF-supported system.

The carbonylation of MeOH/MeI catalysed by **3** was followed by *in situ* high-pressure IR spectroscopy, using a cylindrical internal reflectance (CIR) cell (S2.11, ESI†) as described previously.[11] During the reaction (at 120 °C, 10 bar CO in $CHCl_3$), growth of an absorption at 1741 cm^{-1} was observed (Fig. 3b and Fig S18, ESI†) which corresponds to the ν(C=O) absorption of methyl acetate. This results from carbonylation of MeOH/MeI according to the overall reactions 2MeOH + CO → MeOAc + H_2O or MeOH + MeI + CO → MeOAc + HI. The homogeneous catalytic reaction using *n*-Bu$_4$N$[Rh(CO)_2I_2]$ (with equimolar Rh) was also monitored under identical conditions. The TOF values determined from the slopes of the plots in Fig. 3b for the heterogeneous and homogeneous catalysts are 6.6 h^{-1} and 21.8 h^{-1}, respectively. By comparison, a TOF of ~20 h^{-1} was found in our recent study using a dispersible microporous polymer support.[11] The slower rate for the MOF-supported catalyst may indicate greater diffusion limitations for the MOF. PXRD of the recovered material following catalysis indicates crystallinity of the MOF is maintained (Fig. 2a) and an IR spectrum (Fig. S20, ESI†) shows a ν(CO) band at 2086 cm^{-1} consistent with the presence of the Rh(III) acetyl complex *trans*-$[Rh(CO)_2(COMe)I_3]^-$, as expected upon exposure of $[Rh(CO)_2I_2]^-$ to MeI and CO. Furthermore, a repeat experiment using the solid material recovered from the catalytic run using **3** shows no loss of catalytic activity (Fig. 3b).

In summary, the carbonylation catalyst *cis*-$[Rh(CO)_2I_2]^-$ has been heterogenised in the micropores of a mixed-linker UiO-66-type MOF *via* Coulombic interactions. The encapsulated catalyst is active for the carbonylation of MeOH and can be

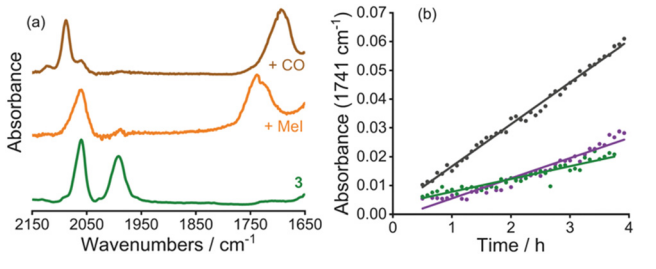

Fig. 3 (a) Infrared spectra (ATR-IR, ν(CO) region) of **3** (green), after soaking in MeI overnight (orange), after exposure to CO atmosphere for 10 days (brown), and (b) growth of ν(CO) absorbance of methyl acetate with time using **3** (green), repeat run using solid recovered from experiment with **3** (purple) and ^{n}Bu$_4$N$[Rh(CO)_2I_2]$ (grey) in $CHCl_3$ at 120 °C (10 bar CO, 0.8 M MeI, 2.5 M MeOH).

recovered and recycled without loss of activity or framework decomposition. IR spectroscopic studies verify formation of the same intermediate Rh species as for the established homogeneous catalytic cycle.

We thank the University of Sheffield for funding a PhD studentship (SAI).

Conflicts of interest

There are no conflicts to declare.

Notes and references

1 K. Shah, *Acetic acid: overview and market outloook*, Indian Petrochem Conference, 2014.
2 A. Haynes, *Advances in Catalysis*, ed. B. C. Gates, H. Knozinger and F. C. Jentoft, 2010, vol. 53, pp. 1–45.
3 D. Förster and T. C. Singleton, *J. Mol. Catal.*, 1982, **17**, 299–314.
4 M. J. Howard, M. D. Jones, M. S. Roberts and S. A. Taylor, *Catal. Today*, 1993, **18**, 325–354.
5 B. L. Smith, G. P. Torrence, M. A. Murphy and A. Aguiló, *J. Mol. Catal.*, 1987, **39**, 115–136.
6 J. H. Jones, *Platinum Met. Rev.*, 2000, **44**, 94–105.
7 A. Haynes, P. M. Maitlis, G. E. Morris, G. J. Sunley, H. Adams, P. W. Badger, C. M. Bowers, D. B. Cook, P. I. P. Elliott, T. Ghaffar, H. Green, T. R. Griffin, M. Payne, J. M. Pearson, M. J. Taylor, P. W. Vickers and R. J. Watt, *J. Am. Chem. Soc.*, 2004, **126**, 2847–2861.
8 R. S. Drago, E. D. Nyberg, A. Elamma and A. Zombeck, *Inorg. Chem.*, 1981, **20**, 641–644.
9 N. Yoneda, T. Minami, J. Weiszmann and B. Spehlmann, *Stud. Surf. Sci. Catal.*, 1999, **121**, 93–98.
10 A. Haynes, P. M. Maitlis, R. Quyoum, C. Pulling, H. Adams, S. E. Spey and R. W. Strange, *J. Chem. Soc., Dalton Trans.*, 2002, 2565–2572.
11 S. A. Ivko, A. M. James, M. J. Derry, R. Dawson and A. Haynes, *Catal. Sci. Technol.*, 2022, **12**, 664–673.
12 A. Bavykina, N. Kolobov, I. S. Khan, J. A. Bau, A. Ramirez and J. Gascon, *Chem. Rev.*, 2020, **120**, 8468–8535.
13 V. Pascanu, G. G. Miera, A. K. Inge and B. Martin-Matute, *J. Am. Chem. Soc.*, 2019, **141**, 7223–7234.
14 M. C. Wasson, C. T. Buru, Z. Chen, T. Islamoglu and O. K. Farha, *Appl. Catal., A*, 2019, **586**, 117214.
15 Y.-S. Wei, M. Zhang, R. Zou and Q. Xu, *Chem. Rev.*, 2020, **120**, 12089–12174.
16 Z. H. Li, T. M. Rayder, L. S. Luo, J. A. Byers and C. K. Tsung, *J. Am. Chem. Soc.*, 2018, **140**, 8082–8085.
17 L. Zhang, Q. B. Cao, F. Gao, Y. P. Dong and X. F. Li, *Polym. Chem.*, 2020, **11**, 2904–2913.
18 D. T. Genna, A. G. Wong-Foy, A. J. Matzger and M. S. Sanford, *J. Am. Chem. Soc.*, 2013, **135**, 10586–10589.
19 D. T. Genna, L. Y. Pfund, D. C. Samblanet, A. G. Wong-Foy, A. J. Matzger and M. S. Sanford, *ACS Catal.*, 2016, **6**, 3569–3574.
20 A. Grigoropoulos, A. I. McKay, A. P. Katsoulidis, R. P. Davies, A. Haynes, L. Brammer, J. Xiao, A. S. Weller and M. J. Rosseinsky, *Angew. Chem., Int. Ed.*, 2018, **57**, 4532–4537.
21 A. Chołuj, A. Zieliński, K. Grela and M. J. Chmielewski, *ACS Catal.*, 2016, **6**, 6343–6349.
22 A. Chołuj, R. Karczykowski and M. J. Chmielewski, *Organometallics*, 2019, **38**, 3392–3396.
23 A. Chołuj, P. Krzesiński, A. Ruszczyńska, E. Bulska, A. Kajetanowicz and K. Grela, *Organometallics*, 2019, **38**, 3397–3405.
24 Y. Liu, X. B. Xi, C. C. Ye, T. F. Gong, Z. W. Yang and Y. Cui, *Angew. Chem., Int. Ed.*, 2014, **53**, 13821–13825.
25 A. Grigoropoulos, G. F. S. Whitehead, N. Perret, A. P. Katsoulidis, F. M. Chadwick, R. P. Davies, A. Haynes, L. Brammer, A. S. Weller, J. L. Xiao and M. J. Rosseinsky, *Chem. Sci.*, 2016, **7**, 2037–2050.
26 J. Y. Ren, P. C. Lan, M. Chen, W. J. Zhang and S. Q. Ma, *Organometallics*, 2019, **38**, 3460–3465.
27 X. Wang, W. Lu, Z.-Y. Gu, Z. Wei and H.-C. Zhou, *Chem. Commun.*, 2016, **52**, 1926–1929.
28 H. D. Park, M. Dincă and Y. Román-Leshkov, *ACS Cent. Sci.*, 2017, **3**, 444–448.
29 H. D. Park, M. Dincă and Y. Román-Leshkov, *J. Am. Chem. Soc.*, 2018, **140**, 10669–10672.
30 A. Burgun, C. J. Coghlan, D. M. Huang, W. Q. Chen, S. Horike, S. Kitagawa, J. F. Alvino, G. F. Metha, C. J. Sumby and C. J. Doonan, *Angew. Chem., Int. Ed.*, 2017, **56**, 8412–8416.
31 J. H. Cavka, S. Jakobsen, U. Olsbye, N. Guillou, C. Lamberti, S. Bordiga and K. P. Lillerud, *J. Am. Chem. Soc.*, 2008, **130**, 13850–13851.
32 M. Kandiah, S. Usseglio, S. Svelle, U. Olsbye, K. P. Lillerud and M. Tilset, *J. Mater. Chem.*, 2010, **20**, 9848–9851.
33 M. Kandiah, M. H. Nilsen, S. Usseglio, S. Jakobsen, U. Olsbye, M. Tilset, C. Larabi, E. A. Quadrelli, F. Bonino and K. P. Lillerud, *Chem. Mater.*, 2010, **22**, 6632–6640.
34 K. Manna, T. Zhang and W. B. Lin, *J. Am. Chem. Soc.*, 2014, **136**, 6566–6569.
35 C. Wang, Z. G. Xie, K. E. deKrafft and W. L. Lin, *J. Am. Chem. Soc.*, 2011, **133**, 13445–13454.
36 J. Liang, R. P. Chen, X. Y. Wang, T. T. Liu, X. S. Wang, Y. B. Huang and R. Cao, *Chem. Sci.*, 2017, **8**, 1570–1575.
37 A. Fulford, C. E. Hickey and P. M. Maitlis, *J. Organomet. Chem.*, 1990, **398**, 311–323.
38 R. J. Adcock, D. H. Nguyen, S. Ladeira, C. Le Berre, P. Serp and P. Kalck, *Inorg. Chem.*, 2012, **51**, 8670–8685.
39 A. Haynes, B. E. Mann, G. E. Morris and P. M. Maitlis, *J. Am. Chem. Soc.*, 1993, **115**, 4093–4100.
40 H. Adams, N. A. Bailey, B. E. Mann, C. P. Manuel, C. M. Spencer and A. G. Kent, *J. Chem. Soc., Dalton Trans.*, 1988, 489–496.